© Federation of European Neuroscience Societies

Long-range oscillatory Ca²⁺ waves in rat spinal dorsal horn

Ruth Ruscheweyh and Jürgen Sandkühler
Department of Neurophysiology, Center for Brain Research, Medical University of Vienna, Vienna, Austria

Abstract

Synchronous activity of large populations of neurons shapes neuronal networks during development. However, re-emergence of such activity at later stages of development could severely disrupt the orderly processing of sensory information, e.g. in the spinal dorsal horn. We used Ca²⁺ imaging in spinal cord slices of neonatal and young rats to assess under which conditions synchronous activity occurs in dorsal horn. No spontaneous synchronous Ca²⁺ transients were detected. However, increasing neuronal excitability by application of 4-aminopyridine after pretreatment of the slice with blockers of (RS)-alpha-amino-3-hydroxy-5-methyl-4-isoxazolepropionic acid (AMPA)/kainate, γ-aminobutyric acid (GABA)ₐ and glycine receptors evoked repetitive Ca²⁺ waves in dorsal horn. These waves spread mediolaterally with a speed of 1.0 ± 0.1 mm/s and affected virtually every dorsal horn neuron. The Ca²⁺ waves were associated with large depolarizing shifts of the membrane potential of participating neurons and were most likely synaptically mediated because they were abolished by blockade of action potentials or *N*-methyl-D-aspartate (NMDA) receptors. They were most pronounced in the superficial dorsal horn and absent from the ventral horn. A significant proportion of the Ca²⁺ waves spread to the contralateral dorsal horn. This seemed to be enabled by disinhibition as primary afferent-induced dorsal horn excitation crossed the midline only when GABAₐ and glycine receptors were blocked. Interestingly, the Ca²⁺ waves occurred under conditions where AMPA/kainate receptors were blocked. Thus, superficial dorsal horn NMDA receptors are able to sustain synchronous neuronal excitation in the absence of functional AMPA/kainate receptors.

Introduction

Spontaneous synchronous activity is a typical feature of developing networks throughout the CNS (O'Donovan *et al.*, 2005). It is present at embryonal and early neonatal stages, and often diminishes or disappears thereafter (Garaschuk *et al.*, 1998, 2000; Peinado, 2001). This seems reasonable because synchronous network activity may be purposeful during early development, promoting neuronal maturation, activity-dependent synaptic wiring and network formation (Katz & Shatz, 1996; Hanse *et al.*, 1997; Feller, 1999; Bregestovski & Spitzer, 2005), but it is obvious that synchronous network activity has to be prevented in more mature animals for the benefit of orderly information processing. However, at developmental stages where spontaneous network activity has ceased, synchronous Ca²⁺ or electrical network activity can often be re-enabled by manipulations that increase neuronal excitability (Aram *et al.*, 1991; Garaschuk *et al.*, 2000).

The spinal dorsal horn is the first site of processing and integration of nociceptive information arriving from the periphery (Willis & Coggeshall, 2004). Sudden simultaneous activation of groups of dorsal horn neurons processing nociceptive information in the intact animal would probably lead to a shooting pain sensation as it is sometimes seen in neuropathic pain. Synchronous activation of larger parts of the dorsal horn network would lead to pain that violates the innervation patterns of peripheral nerves or dorsal roots, another feature of neuropathic pain (Maleki *et al.*, 2000; Jensen *et al.*, 2001). Therefore, it is important to understand how synchronous network activity in the spinal dorsal horn can be evoked at developmental stages where it is normally not present, and what mechanisms

contribute to prevent it. In addition, the properties of synchronous activity may provide insights into the function of the dorsal horn network. Previous studies suggest that synchronized network activity may occur in the spinal dorsal horn under certain conditions, but their methods did not allow the determination of the number and distribution of the participating neurons (Czéh & Somjen, 1989; Lidierth & Wall, 1996; Kremer & Lev-Tov, 1998; Demir *et al.*, 2002; Ruscheweyh & Sandkühler, 2003; Asghar *et al.*, 2005).

Here we used Ca²⁺-imaging techniques to simultaneously monitor the activity of large populations of spinal dorsal horn neurons. Synchronous neuronal activity leading to oscillatory Ca²⁺ waves was evoked in the spinal dorsal horn network by the potassium channel blocker 4-aminopyridine (4-AP) after pretreatment with blockers of γ-aminobutyric acid (GABA)ₐ, glycine and (RS)-alpha-amino-3-methyl-4-isoxazolepropionic acid (AMPA)/kainate receptors. Possible pathophysiological implications of the synchronous spinal dorsal horn neuronal activity for sensory processing are discussed.

Materials and methods

Preparation of spinal cord slices

Sprague–Dawley rats of three age groups [postnatal day (P) 5–7, P10–12 and P16–19] were killed by decapitation under deep ether anaesthesia and the lumbar spinal cord was removed. Four-hundred−500-μm-thick transverse slices, for some experiments with an attached dorsal root (4–10 mm long), were cut on a microslicer (DTK-1000, Dosaka, Kyoto, Japan) and stored in an incubation solution (in mм: NaCl, 95; KCl, 1.8; KH₂PO₄, 1.2; CaCl₂, 0.5; MgSO₄, 7; NaHCO₃, 26; glucose, 15; sucrose, 50; oxygenated with 95% O₂, 5% CO₂; pH 7.4, measured osmolality 310–320 mOsmol).

Correspondence: Dr J. Sandkühler, as above.
E-mail: juergen.sandkuehler@meduniwien.ac.at

All animal experiments were in accordance with European Communities Council directives (86/609/EEC) and were approved by the Austrian Federal Ministry for Education, Science and Culture.

Fluorometric Ca²⁺ measurements

For Ca^{2+} measurements, slices were incubated for 30 min at room temperature (20–24 °C) in incubation solution containing fura 2 acetoxymethyl ester (fura-2 AM, 10 μM), followed by a ≥30-min wash-out period in normal incubation solution. A single fura-2-loaded slice was then placed in a recording chamber mounted on an upright microscope (Olympus BX50WI, Olympus, Japan) where it was superfused by recording solution at 3 mL/min at room temperature. Recording solution was identical to incubation solution except for (in mM): NaCl, 127; $CaCl_2$, 2.4; $MgSO_4$, 1.3; sucrose, 0. Slices were illuminated with a monochromator and images were captured with a cooled CCD camera (TILL Photonics, Gräfelfing, Germany) at rates between 1 and 33 Hz. In most experiments, paired exposures to 340 and 380 nm were obtained, and the ratio (F_{340}/F_{380}) was calculated to assess changes in relative Ca^{2+} concentration without conversion to absolute concentration values. To achieve recordings at high frame rates (33 Hz), only 380-nm exposures were made, and rises in Ca^{2+} concentrations were detected as a decline in the fluorescence intensity. Changes in Ca^{2+} concentration were either evaluated in single cells by placing a small region of interest over the cell body or in larger areas comprising many cells by averaging the fluorescence of the whole area, including the background that was composed by both non-cellular sources and cells that were out of focus because of their location deep in the slice. Synchrony between Ca^{2+} signals from different cells was determined by correlation analysis. A Ca^{2+} transient was considered significant when its amplitude exceeded four times the root mean square value of the baseline fluorescence of the respective area of interest, and the corresponding point in time was defined as the onset of the Ca^{2+} transient. A neuron was judged to participate in a given population Ca^{2+} transient if it exhibited a significant Ca^{2+} transient with the same onset (within the temporal resolution of 1 s) as the population Ca^{2+} transient under study.

Patch-clamp recording

Fura-2-loaded or naïve slices were placed in the recording chamber and superfused by recording solution. Dorsal horn neurons were visualized with Dodt-infrared optics (Dodt *et al.*, 1998) and recorded in the whole-cell patch-clamp configuration with glass pipettes (2–6 MΩ) filled with internal solution (in mM: potassium gluconate, 120; KCl, 20; $MgCl_2$, 2; Na_2ATP, 2; NaGTP, 0.5; HEPES, 20; EGTA, 0.5; pH 7.28 with KOH, measured osmolality 300 mOsmol) as described elsewhere (Ruscheweyh & Sandkühler, 2002). Voltage- and current-clamp recordings were made using an Axopatch 200B amplifier and the pCLAMP 8 or 9 acquisition software (Axon Instruments, Union City, CA, USA). Signals were low-pass filtered at 2–5 kHz, amplified fivefold, sampled at 5–10 kHz and analysed offline using pCLAMP 9.

Primary afferent stimulation

The dorsal root was stimulated through a suction electrode with a constant current stimulator (WPI, Sarasota) at 0.1 ms pulse width.

Statistical analysis

All values are means ± SEM. The non-parametric Mann–Whitney and Wilcoxon rank-sum tests, ANOVA on ranks followed by a Mann–Whitney test corrected by the Bonferroni adjustment, the Pearson Product Moment correlation and cross-correlation plots were used for statistical comparisons where appropriate.

Drugs

Drugs and their sources were as follows: 4-aminopyridine (4-AP, 100 μM), (–)-bicuculline methiodide (bicuculline, 10 μM), strychnine (4 μM) and cyclopiazonic acid (30 μM) were from Sigma (Deisenhofen, Germany), D-2-amino-5-phosphonovaleric acid (D-AP5, 50 μM), 6-cyano-7-nitro-quinoxaline-2,3-dione (CNQX, 10 μM), tetrodotoxin (TTX, 1 μM) and thapsigargin (2 μM) were from Alexis (Grünstadt, Germany). (+)-MK 801 maleate (MK 801, 20 μM) was from Tocris (Bristol, UK) and fura-2 AM was from Molecular Probes (Leiden, the Netherlands). Stock solutions were prepared by dissolving bicuculline, MK 801 and D-AP5 in distilled water; strychnine, CNQX, cyclopiazonic acid, thapsigargin and fura-2 AM in dimethyl sulphoxide (Sigma) and TTX in acidic buffer (pH 4.8) and stored in aliquots at −20 °C. Drugs were added to the superfusion solution at defined concentrations as indicated.

Results

Loading with fura-2 AM produced distinct staining of many cell bodies and proximal processes throughout the spinal cord grey matter. Patch-clamp recordings from stained dorsal horn cells revealed that they were neurons in every case ($n = 16$), so that we suppose that the vast majority of stained cells in the dorsal horn were neurons. To assess the presence of synchronous Ca^{2+} signals in the spinal dorsal horn of a slice, a region encompassing the medial or middle third of the superficial dorsal horn (including lamina II and variable parts of laminae I and III) was imaged (e.g. Fig. 1A). This allowed simultaneous imaging of several 10s of fura-2-loaded cell bodies (see Fig. 1B for an example). Where not stated otherwise, a frame rate of 1 Hz was used.

Lack of spontaneous network Ca²⁺ transients in neonatal rat spinal dorsal horn

To investigate if spontaneous synchronized Ca^{2+} transients occur in the spinal dorsal horn network, Ca^{2+}-imaging was performed in slices at different developmental stages (P5–7, $n = 3$ and P10–12, $n = 3$) for 60 min. Although spontaneous Ca^{2+} transients frequently occurred in single neurons, no synchronous rises of Ca^{2+} in major subpopulations of cells were encountered. Occasionally (0–2 times in a 60-min observation period), simultaneous Ca^{2+} transients were detected in small ensembles of two–six cells.

Network Ca²⁺ transients evoked by disinhibition

As in many neuronal networks spontaneous synchronized activity arises when synaptic inhibition is removed (Müller & Misgeld, 1991; Bracci *et al.*, 1996); we tested the effect of blockers of $GABA_A$ and glycine receptors (bicuculline 10 μM and strychnine 4 μM, added to the recording solution ≥15 min before starting the Ca^{2+}-imaging). Spontaneous network Ca^{2+} transients were indeed observed under these conditions at a low rate (0.1 ± 0.1 transients/min, $n = 5$ slices, P10–12, data not shown) with a high variance in rate (1–27 transients per hour) and in the number of neurons in the imaged field participating in
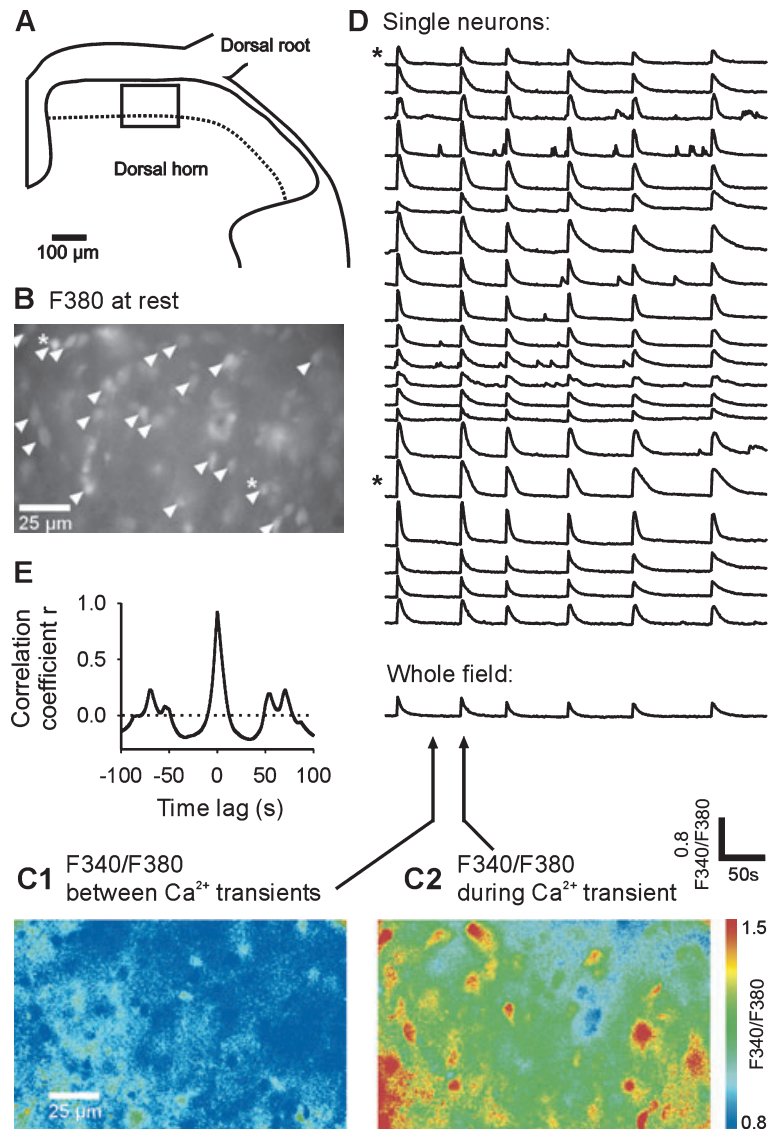
FIG. 1. Synchronous Ca^{2+} oscillations in spinal dorsal horn evoked by 4-AP. A slice from an 11-day-old rat was preincubated with CNQX (10 μM), bicuculline (10 μM) and strychnine (4 μM). After addition of 4-AP (100 μM) to the bath, Ca^{2+} oscillations occurred synchronously in most dorsal horn neurons. (A) The box superimposed to the outline of the dorsal horn delimits the region selected for imaging. Dotted line, approximate border between lamina II and III. (B) The selected superficial dorsal horn region contained multiple fura-2-loaded cells shown at 380 nm illumination before the addition of 4-AP. Arrowheads point to 20 neurons that were selected for detailed analysis of their Ca^{2+} gradients. (C) The ratio of the images captured at 340 and 380 nm illumination was used to detect changes in intracellular Ca^{2+} concentration. Examples of the ratio image between Ca^{2+} oscillations (C1) and during a population Ca^{2+} transient (C2) are shown in pseudocolour. While Ca^{2+} was uniformly low between transients, Ca^{2+} was simultaneously elevated in most of the imaged neurons during the transient. (D) Original traces show the time course (456–876 s after application of 4-AP) of the Ca^{2+} concentration of the neurons marked in (A). The bottom trace illustrates the changes in Ca^{2+} concentration averaged over the whole section shown in (B). Several transient elevations in intracellular Ca^{2+} concentration that were synchronized among all illustrated neurons and reflected in the whole-field Ca^{2+} activity are evident. Some neurons additionally showed smaller standalone Ca^{2+} transients, corresponding to spontaneous activity of single cells. (E) Cross-correlogram of the Ca^{2+} traces of the two cells marked by asterisks in (B) and (D).

the transient (11–97%; mean: 56 ± 12%; the imaged field included 47–59 neurons). The occurrence of spontaneous network Ca^{2+} transients in the presence of bicuculline and strychnine was reduced by addition of the blocker of AMPA/kainate receptors, CNQX (10 μM, rate 0.01 ± 0.00 transients/min, 22 ± 0% of neurons in the imaged field participated, $n = 5$ slices, P10–12, the imaged field included 41–57 neurons, data not shown).

Network Ca^{2+} oscillations evoked by 4-AP

Addition of 4-AP to the bath solution turned out to increase the rate of synchronous Ca^{2+} transients and largely decrease the variability of

results between slices. Repetitive transient Ca^{2+} elevations (Ca^{2+} oscillations) that occurred synchronously within the 1-Hz time resolution in most of the neurons encompassed by the imaged region were reliably induced by addition of 4-AP (100 μM) to the bath solution of slices that had been incubated with CNQX, bicuculline and strychnine (10 μM, 10 μM and 4 μM) for ≥15 min (Fig. 1). Synchronous Ca^{2+} transients were similar in shape to the spontaneously occurring asynchronous Ca^{2+} transients, displaying a steep rise and slower decay, with a return to near baseline values within 10–30 s (Fig. 1D). Synchrony of the Ca^{2+} signals between arbitrarily selected neurons in the imaged field was confirmed by cross-correlation plots that showed distinct peaks at zero time lag (see Fig. 1E for an

example). Correlation analysis between pairs of cells in the imaged field yielded significant correlations in 98% of the tests with coefficients (r) between 0.31 and 0.99 (10 slices, 20 cells arbitrarily selected per slice, 1867/1900 correlations significant with $P < 0.01$ after Bonferroni correction). As each imaged region contained large numbers of neurons participating in the repetitive synchronous activity, this activity was apparent also when the change of fluorescence was averaged over the whole imaged field (Fig. 1D, bottom trace). The quantification of the synchronous activity and, where not indicated otherwise, the original traces shown in the figures were derived from the fluorescence signal averaged over the whole imaged field.

Age dependency

The onset and characteristics of the synchronous Ca^{2+} oscillations were clearly age dependent. Without aiming at a full developmental characterization of the phenomenon, we investigated the synchronous Ca^{2+} activity in three different age groups (P5–7, $n = 15$; P10–12, $n = 26$; P16–19, $n = 13$). The middle age group showed the earliest onset of the synchronous Ca^{2+} activity after application of 4-AP (Fig. 2; P5–7, 573 ± 48 s, $n = 15$; P10–12, 416 ± 28 s, $n = 26$; P16–17, 980 ± 111 s, $n = 7$) and was therefore selected for all further experiments. The rate of synchronous Ca^{2+} transients was difficult to obtain because in the P5–7 and P16–19 age groups only small numbers of Ca^{2+} transients were present during the 15–30-min observation period that started after application of 4-AP. The instantaneous frequency calculated from the first two Ca^{2+} transients, where available, was as follows: P5–7, 0.5 ± 0.1 events/min, $n = 14$; P10–12, 1.2 ± 0.1 events/min, $n = 26$; P16–17, 1.0 ± 0.2 events/min, $n = 5$, $P < 0.01$ for the comparison between P5–7 and P10–12. The coefficient of variation of the Ca^{2+} transient instantaneous frequency, an indicator for the oscillation regularity, was calculated from the first five Ca^{2+} transients where available, and was not significantly different between age groups (P5–7, 0.16 ± 0.06, $n = 2$; P10–12, 0.23 ± 0.03, $n = 23$; P16–17, 0.25 ± 0.03, $n = 4$). While typical synchronous Ca^{2+}

transients, albeit often with a quite late onset of the activity, could be observed at P16–17, results were highly variable at P19 ($n = 6$). At this age, most Ca^{2+} transients were synchronous only in limited and variable subgroups (~ 5–50%) of the observed neurons and therefore not regularly visible in the whole-field analysis.

Virtually all superficial dorsal horn cells participate in the synchronous Ca^{2+} oscillations

As illustrated in Fig. 1D, a high proportion of the neurons included in the imaged region participated in the synchronous Ca^{2+} oscillations. To quantify this proportion, we analysed five synchronous Ca^{2+} transients per slice in 10 slices. We arbitrarily selected 30 fura-2-loaded neurons per slice from the 380-nm baseline exposure and compared their Ca^{2+} signals with the synchronous population Ca^{2+} transients extracted from the whole-field fluorescence. All of the analysed neurons participated in the synchronous network Ca^{2+} oscillations. Rarely, failures to participate in a specific Ca^{2+} transient were observed. Altogether, the selected neurons participated in $97 \pm 2\%$ ($n = 10$ slices) of the Ca^{2+} transients.

Neuronal activity associated with network Ca^{2+} oscillations

Patch-clamp recordings obtained in or near the region selected for imaging showed that network Ca^{2+} transients were correlated with large (peak amplitude 280 ± 94 pA), slow (10–90% rise time: 145 ± 31 ms; 90–37% decay time: 509 ± 184 ms) inward membrane currents in single neurons ($n = 5$ slices, one neuron per slice was recorded in the patch-clamp configuration, P10–12, a total of 72 Ca^{2+} transients were recorded, see Fig. 3A and B for examples). The onset of the slow inward currents (414 ± 28 s after addition of 4-AP) coincided with that of the Ca^{2+} transients, and no slow inward currents were recorded out of phase with the population Ca^{2+} activity. In some neurons, small inward currents appeared between the large current transients (see Fig. 3A for an example) that were similar in size, shape and kinetics to unitary spontaneous synaptic currents. These currents almost completely disappeared together with the large transients after application of the NMDA receptor blocker MK 801 and were not investigated further. When recorded in current-clamp, neurons fired action potentials with a rate of up to 30 Hz during the depolarizing shift associated with population Ca^{2+} transients (19 Ca^{2+} transients from two slices, one neuron per slice was recorded in the patch-clamp configuration, see Fig. 3C for an example). Repetitive slow membrane currents similar in shape, onset and rate were observed in patch-clamp recordings from slices that were not loaded with fura-2 and not exposed to the imaging illumination, demonstrating that the population oscillations were not side-effects of the staining or imaging procedure.

Time course of the synchronous network activity

As photobleaching makes it difficult to record Ca^{2+} concentrations with high temporal and spatial resolution over prolonged periods of time, we relied on population Ca^{2+} transient-associated membrane currents recorded from single neurons to determine the time course of the synchronous network activity. Ca^{2+} transient-associated membrane currents persisted throughout the first hour after application of 4-AP with a significant decline in rate (1.4 ± 0.3 events/min at onset of the activity, 0.8 ± 0.1 events/min after 1 h, frequencies calculated from five consecutive events, $n = 6$ slices, one neuron recorded per slice, $P < 0.05$, see Fig. 3D for an example).
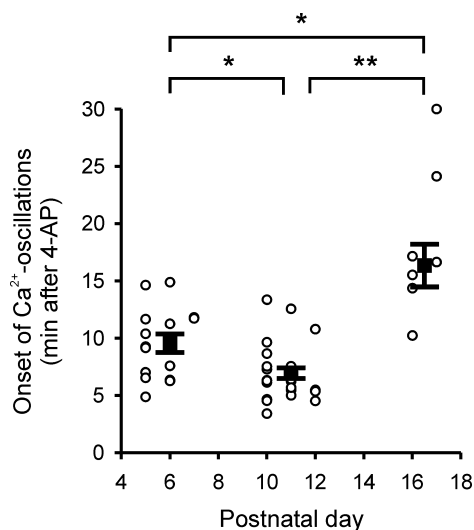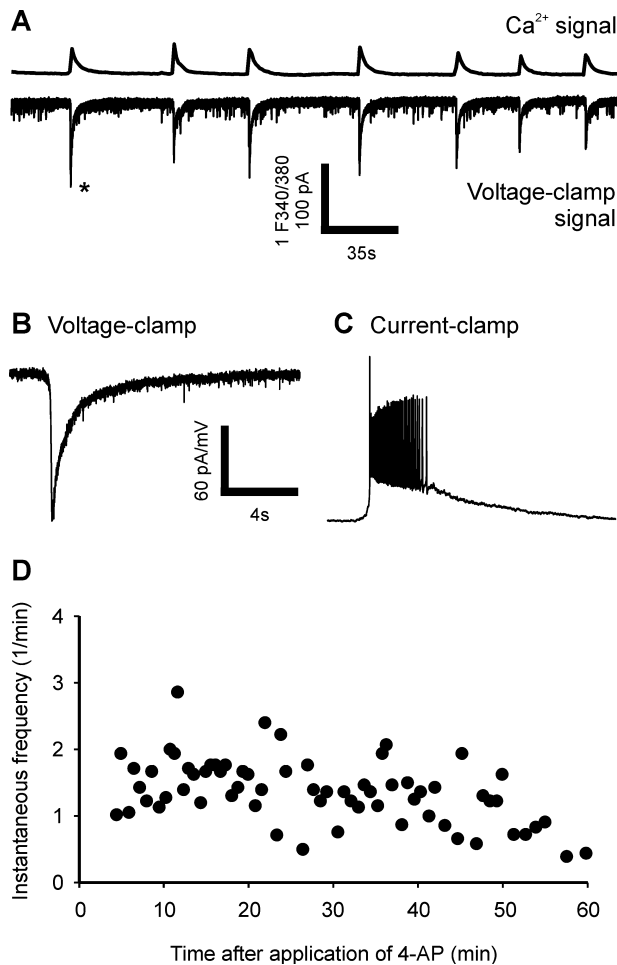

FIG. 2. Age dependency of spinal dorsal horn population Ca^{2+} oscillations. Three age groups are shown: postnatal day (P) 5–7, P10–12 and P16–17. The onset of population Ca^{2+} oscillations after addition of 4-aminopyridine (4-AP) to the bath is illustrated, every circle representing one experiment. Black symbols indicate mean value and standard error of the respective age group. **$P < 0.01$; *$P < 0.05$.

FIG. 3. Electrophysiological correlates and time course of the spinal dorsal horn population Ca²⁺ oscillations. (A) Parallel recording of the population Ca²⁺ concentration and whole-cell membrane currents of a single neuron inside the imaged region. Each population Ca²⁺ transient was reflected by a slow inward current in the single-cell recording. An amplification of the inward current marked by a star is displayed in (B). (C). When the same neuron was recorded in current-clamp mode, population Ca²⁺ transients correlated with large depolarizing shifts with superimposed action potentials. (D) Time course of the synchronous network activity, obtained by evaluation of the population Ca²⁺ transient-associated membrane currents in a 1-h patch-clamp recording. The instantaneous frequency at a given time point was calculated from the distance between two adjacent Ca²⁺ transient-associated membrane currents.

Each network Ca²⁺ transient represents a wave of activity spreading over the dorsal horn

Regions of interest encompassing the entire mediolateral extent of the superficial dorsal horn were selected and imaged at a frame rate of 33 Hz (Fig. 4A). A total of 20 Ca²⁺ transients from five slices were analysed. At this temporal resolution, propagation of the wavefront was evident in the whole-field fluorescence recordings (Fig. 4B). For a more precise analysis, the Ca²⁺ transient onset was determined for 15 neurons selected along a mediolateral line (Fig. 4A) and plotted against the distance of the cell from the most medial cell (Fig. 4C–E). All these plots could be fitted with one or two linear regressions, as shown in Fig. 4C–E. Eight of the 20 Ca²⁺ transients started at the medial border of the superficial dorsal horn grey matter and propagated laterally, while two started at the lateral border and propagated medially. In 10 of the 20 Ca²⁺ transients, the site of initiation lay in an intermediate region of the superficial dorsal horn

and the Ca²⁺ wave propagated in both directions. The speed of propagation derived from the linear regression was 1.0 ± 0.1 mm/s and not significantly different between lateral and medial propagation. When the propagation was recorded and analysed in the vertical direction, across dorsal horn laminae I to VI (12 Ca²⁺ transients in three slices, not shown), with one exception, linear regression was not successful because the Ca²⁺ transients were detected in all laminae almost simultaneously or showed no clear direction of propagation. It was remarkable that the Ca²⁺ transients were most pronounced in superficial dorsal horn neurons with successively declining amplitudes towards deeper laminae neurons. Imaging in the grey matter of the ventral horn revealed no synchronous Ca²⁺ transients in response to 4-AP in spite of healthy aspect and satisfactory fura-2 staining of ventral horn neurons ($n = 5$ slices, not shown).

Transmission of Ca²⁺ waves and neuronal excitation between left and right dorsal horn

Imaging at low amplification allowed to simultaneously observe Ca²⁺ activity in both dorsal horns of a slice (Fig. 5). After addition of 4-AP, both dorsal horns developed network Ca²⁺ oscillations. While some Ca²⁺ transients occurred independently (delay of 8–127 s between neighbouring transients on the left and right side of the dorsal horn), others appeared in short succession first in one and then in the other dorsal horn (delay 1–2 s, consistent with the time needed to cover the distance of ~ 1000–1500 μm that separates the superficial dorsal horns via the posterior commissure at a conduction velocity of 1 mm/s), with either side being able to lead the excitation (Fig. 5A). Altogether, $41 \pm 12\%$ of the observed Ca²⁺ transients were apparently transmitted between left and right dorsal horn, with a strong variability between slices (range 10–91%, six slices, a total of 145 Ca²⁺ transients on both sides were evaluated).

To investigate under which conditions strong excitation of the superficial dorsal horn network is able to cross the midline and invade the contralateral dorsal horn, we used a different experimental design. We excited dorsal horn cells by electrical stimulation of the dorsal root for 1 s at 100 Hz using a supramaximal intensity (3 mA, 0.5 ms) at 5-min intervals. This produced population Ca²⁺ transients of similar amplitude and kinetics as the 4-AP-evoked transients (amplitude recorded at $4 \times$ optical magnification: dorsal root stimulation: 0.051 ± 0.012 F_{340}/F_{380}, $n = 3$ slices, nine transients; 4-AP: 0.063 ± 0.019 F_{340}/F_{380}, $n = 5$ slices, 25 transients; rise time: below the temporal resolution of 1 s; 90–37% decay time: dorsal root stimulation: 5 ± 1 s; 4-AP: 4 ± 1 s, all comparisons not significant). In drug-free recording solution (i.e. in the absence of 4-AP and blockers of synaptic transmission), these population Ca²⁺ transients were limited to the ipsilateral dorsal horn (three slices, nine stimulations, see Fig. 5B for an example). In contrast, after addition of the GABA_A and glycine receptor antagonists bicuculline (10 μM) and strychnine (4 μM) to the recording solution, dorsal root stimulation in most cases evoked pronounced Ca²⁺ transients bilaterally (three slices, 17/20 stimulations evoked contralateral Ca²⁺ signals, see Fig. 5C for an example). This suggests that pathways between both dorsal horns are tonically inhibited by GABA and/or glycine.

Pharmacology of network Ca²⁺ oscillations

The present study describes synchronous Ca²⁺ oscillations evoked by 4-AP in the presence of blockers of AMPA/kainate, glycine and GABA_A receptors. When 4-AP is applied in the absence of these blockers, patch-clamp recordings show the previously described
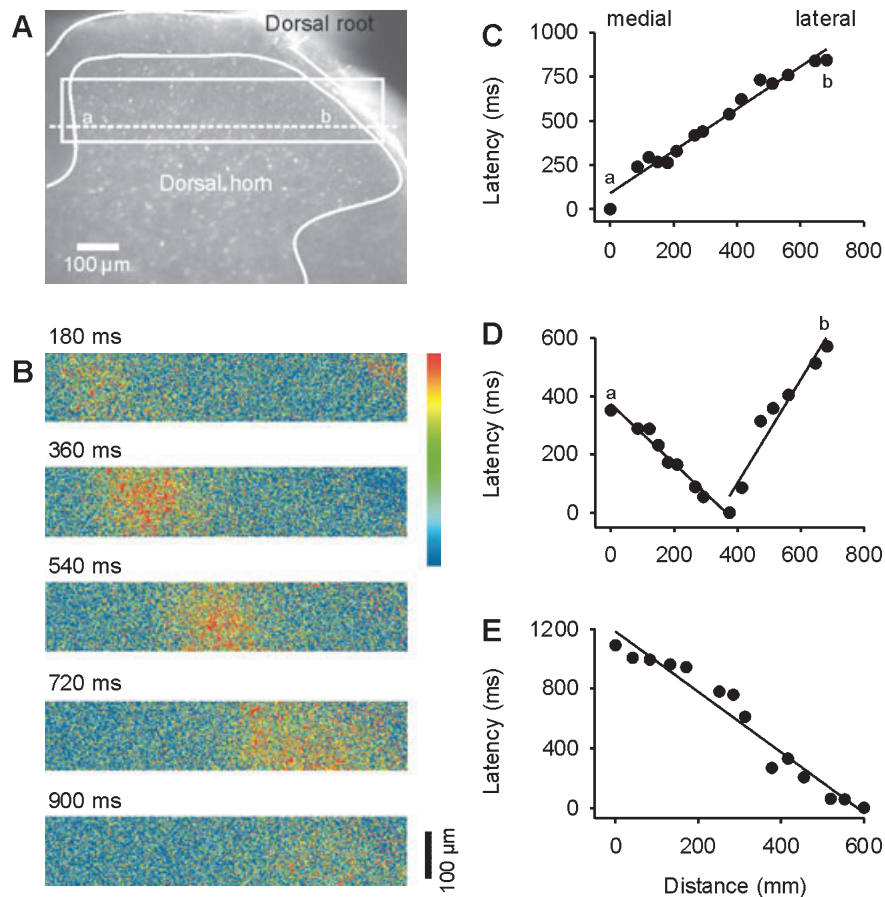
FIG. 4. Initiation and propagation of Ca²⁺ waves in the superficial dorsal horn. (A) A spinal slice section is shown at 380 nm illumination with a superimposed outline of the dorsal horn. Fura-2-loaded cells are visible as small bright spots. (B) A sequence of images taken of the region indicated by the box in (A) during a population Ca²⁺ transient is shown. To highlight the wavefront moving over the spinal dorsal horn, the difference between the 380 nm image at the indicated point in time and the image obtained 180 ms before was calculated and is displayed in pseudocolour. On the colour scale, red indicates large changes of fluorescence while blue indicates small or no change. The points in time indicated above the images correspond to the time scale in (C) that illustrates the same Ca²⁺ wave as (B). (C and D) The time courses of two different Ca²⁺ waves recorded from the slice shown in (A) are illustrated. Fifteen neurons lying near the dashed line in (A) were selected, and the onset of their individual Ca²⁺ transients during a population transient were analysed. The latency relative to the neuron with the earliest onset was then plotted against the distance from the most medial neuron, and the plots were fitted by linear regression. The mediolateral location of the neurons marked with a and b is shown in (A). (E) A lateromedially propagating wave from another slice. Examples (C–E) illustrate that population Ca²⁺ waves can be initiated at various sites in superficial dorsal horn and propagate laterally as well as medially.

(Ruscheweyh & Sandkühler, 2003) 1/s epileptiform network activity, which is reflected by an early, single, slow Ca²⁺ transient ($n = 5$, see Fig. 6A for an example). The single epileptiform discharges evident in patch-clamp recordings were not detectable by Ca²⁺-imaging even at high frame rates, probably reflecting slow elimination of Ca²⁺ from the cytoplasm after strong membrane excitation. With CNQX present in the bath, a late, slow increase in Ca²⁺ concentration with superimposed small synchronous Ca²⁺ transients that were difficult to delimit was induced by 4-AP ($n = 6$, see Fig. 6B for an example). If the slice was pretreated with bicuculline and strychnine alone, 4-AP evoked early, high-rate, small-amplitude synchronous Ca²⁺ transients that were difficult to separate from each other ($n = 3$, see Fig. 6C for an example). Finally, 4-AP in the presence of CNQX, bicuculline and strychnine evoked the presently investigated late-onset, large-amplitude and clearly delimited synchronous Ca²⁺ oscillations (see Fig. 6D for an example). In conclusion, synchronous network Ca²⁺ oscillations in the superficial dorsal horn can be evoked under various experimental conditions but are especially pronounced in the presence of blockers of AMPA/kainate, glycine and GABA$_A$ receptors.

Thus, large network Ca²⁺ oscillations can be evoked when most of the fast chemical synaptic transmission is blocked. Nonetheless, chemical synaptic transmission seems to be necessary for the synchronized Ca²⁺ oscillations given that they were blocked in the presence of the Na⁺ channel blocker TTX (1 μM, $n = 5$, see Fig. 6E for an example) or antagonists at the NMDA receptor (D-AP5, 50 μM, $n = 4$ or MK 801, 20 μM, $n = 6$, see Fig. 6F for an example). The block was complete for TTX and D-AP5. With MK 801, one synchronous Ca²⁺ transient was detected in the six slices tested. As NMDA receptors are Ca²⁺ channels, it is conceivable that blockade of NMDA receptors prevented detection of ongoing synchronous network activity by Ca²⁺-imaging. However, patch-clamp recordings performed in parallel with the Ca²⁺-imaging showed no signs of ongoing network activity in the presence of MK 801 ($n = 3$, not shown). Ca²⁺ oscillations are classified by the contribution of Ca²⁺ from intracellular stores (Berridge & Dupont, 1994). Here, depletion of intracellular stores by thapsigargin (2 μM, $n = 3$) or cyclopiazonic acid (30 μM, $n = 3$, see Fig. 6G for an example) did not significantly alter the onset of the network activity (control: 416 ± 28 s after addition of 4-AP, $n = 26$; thapsigargin/CPA: 409 ± 45 s, $n = 6$), the

number of synchronous Ca^{2+} transients encountered in the first 20 min (control: 13 ± 2, $n = 23$; thapsigargin/CPA: 7 ± 1, $n = 6$) or the oscillation regularity (coefficient of variation: control: 0.23 ± 0.03, $n = 23$; thapsigargin/CPA: 0.36 ± 0.08, $n = 6$) after application of 4-AP.

NMDA receptor-mediated Ca²⁺ signals can be evoked in superficial dorsal horn by synaptic glutamate release

The presently described Ca^{2+} oscillations are dependent on activation of NMDA receptors. At resting membrane potential, NMDA receptors are generally assumed to be blocked by Mg^{2+} ions, which are removed

only if the membrane is concurrently depolarized, e.g. by activation of AMPA/kainate receptors. In the present study, activation of NMDA receptors occurred while much of the fast synaptic transmission through other receptors, including AMPA/kainate receptors, was blocked. We used a different approach to confirm that NMDA receptors in superficial dorsal horn indeed respond to synaptic glutamate release in the presence of AMPA/kainate receptor antagonists. Synaptic glutamate release was achieved by supramaximal electrical stimulation (3 mA, 0.5 ms) of the dorsal root for 1 s at 100 Hz. In drug-free recording solution (i.e. in the absence of 4-AP and blockers of synaptic transmission), this evoked a large population Ca^{2+} transient in superficial dorsal horn. Repetition of the stimulation at 15-min intervals produced Ca^{2+} transients of slightly declining amplitude (Fig. 7, $n = 4$ slices). In the presence of the AMPA/kainate receptor antagonist CNQX (10 μM), the Ca^{2+} transient was significantly reduced but not abolished. CNQX at that concentration completely blocks AMPA/kainate receptor-mediated currents evoked in spinal dorsal horn neurons by supramaximal primary afferent stimulation (unpublished data). When the $GABA_A$ and glycine receptor blockers bicuculline (10 μM) and strychnine (4 μM) were then added to the solution (with CNQX still present), dorsal root stimulation evoked a Ca^{2+} transient that was significantly larger than control. This Ca^{2+} transient was largely NMDA receptor-mediated as it was nearly abolished by D-AP5 (50 μM, $n = 5$ slices, Fig. 7). This demonstrates that synaptic glutamate release can activate spinal dorsal horn NMDA receptors during block of AMPA/kainate receptors. The large potentiation of the NMDA receptor-mediated Ca^{2+} transient by bicuculline and strychnine suggests that tonic release of GABA and glycine keeps superficial dorsal horn neurons hyperpolarized.
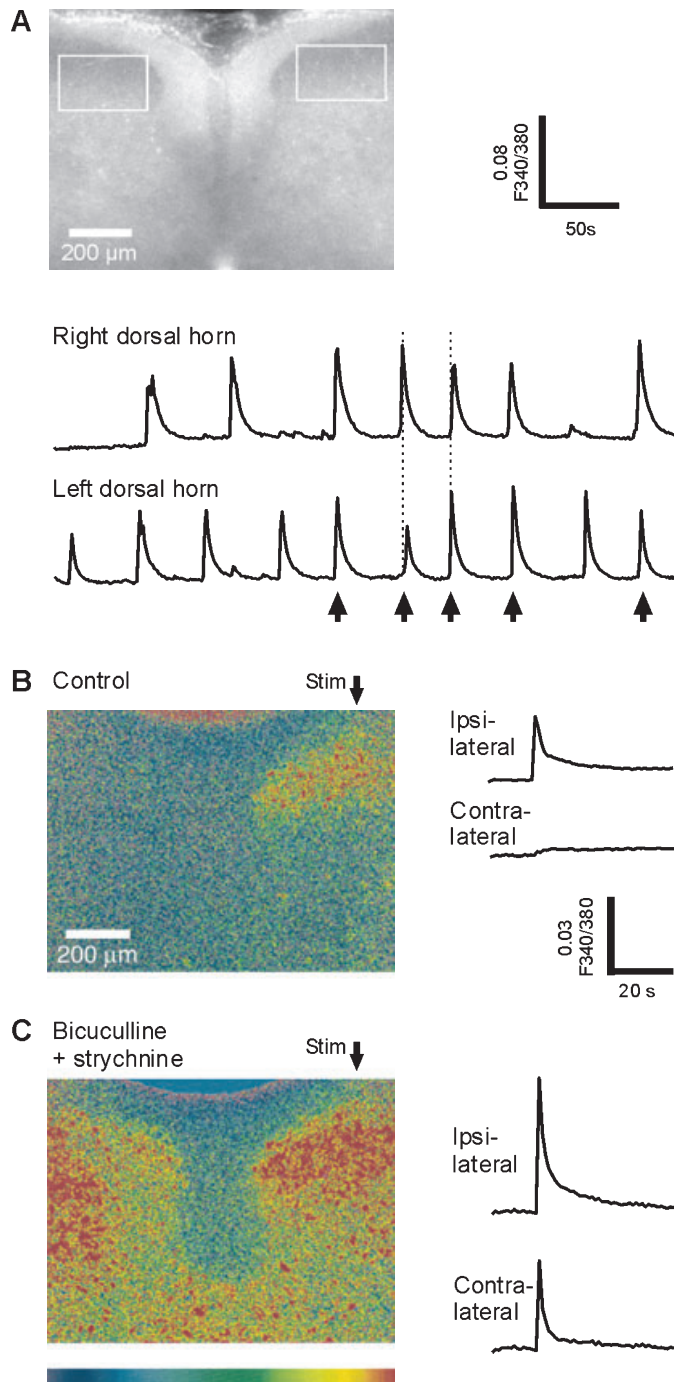
Discussion

This is, to the best of our knowledge, the first description of Ca^{2+} waves spreading over mammalian spinal dorsal horn. These Ca^{2+} waves occurred spontaneously and repetitively in the presence of blockers of AMPA/kainate, $GABA_A$ and glycine receptors and the convulsant drug 4-AP, and engaged the vast majority of lamina I–III dorsal horn neurons. A considerable proportion of the Ca^{2+} waves crossed the midline and reached the contralateral dorsal horn. Ca^{2+} waves were associated with large depolarizing shifts of the membrane potential and action potential firing of dorsal horn neurons.

Fig. 5. Spread of excitation to the contralateral dorsal horn. (A) Transmission of Ca^{2+} waves between the left and right dorsal horn. The transmitted light picture shows a section of the dorsal half of a spinal transversal slice. Boxes indicate the regions in the left and right superficial dorsal horn where simultaneous analysis of Ca^{2+} concentrations was performed. The original Ca^{2+} concentration traces illustrate that some population Ca^{2+} transients occurred independently in left and right dorsal horns while others were near-synchronized between both sides (arrows). Dashed vertical lines show that the Ca^{2+} wave could be initiated in either dorsal horn and reached the opposite side with a delay of 1–3 s. (B, C) In a separate set of experiments, excitation of the dorsal horn network was evoked by electrical stimulation (0.5 ms, 3 mA; 100 Hz for 1 s) of one dorsal root in the absence of 4-AP. The colour images show a dorsal horn section equivalent to that illustrated in (A). The difference of the fluorescence ratio images taken immediately after and before stimulation was calculated and is displayed in pseudocolour. On the colour scale, red indicates large changes of fluorescence while blue indicates small or no change. Next to the pseudocolour images, original Ca^{2+} concentration traces obtained from the ipsilateral (i.e. on the side of the stimulated dorsal root) and contralateral dorsal horn are shown. In drug-free recording solution (B), unilateral stimulation of the dorsal root evoked an excitation limited to the ipsilateral dorsal horn. After addition of bicuculline (10 μM) and strychnine (4 μM) to the bath, unilateral dorsal root stimulation evoked bilateral Ca^{2+} transients (C).
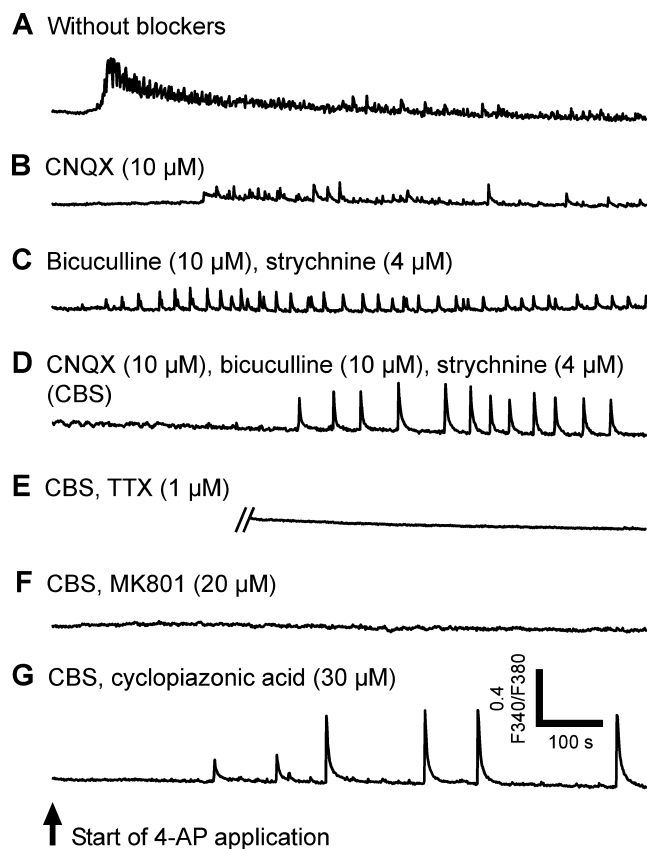
FIG. 6. Pharmacology of spinal dorsal horn population Ca^{2+} oscillations. The effect of 4-aminopyridine (4-AP) application on the population Ca^{2+} concentration in the presence of different combinations of blockers of synaptic transmission (CNQX for AMPA/kainate receptors, bicuculline and strychnine for $GABA_A$ and glycine receptors, MK 801 for NMDA receptors), during blockade of action potentials by tetrodotoxin (TTX) and after depletion of the intracellular Ca^{2+} stores by cyclopiazonic acid was investigated. CBS designates the combination of CNQX (10 μM), bicuculline (10 μM) and strychnine (4 μM). The indicated combination of drugs was washed in for ≥ 15 min before starting the experiment. Original traces (A–G) illustrate the population Ca^{2+} concentration for 15 min after application of 4-AP (100 μM). The recordings under TTX were started 5 min after wash-in of the 4-AP, a time point where Ca^{2+} oscillations are normally already present or about to begin.

FIG. 7. Primary afferent stimulation induces NMDA receptor-mediated population Ca^{2+} transients in the absence of functional AMPA/kainate receptors. Tetanic stimulation (100 Hz, 1 s) of the dorsal root at high intensity (0.5 ms, 3 mA) evoked population Ca^{2+} transients in superficial dorsal horns of drug-free slices. The amplitude of these Ca^{2+} transients declined with repetitive stimulation at 15-min intervals (open symbols, $n = 4$ slices). Closed symbols show amplitudes of Ca^{2+} transients in drug-free solution and after successive addition of the AMPA/kainate receptor antagonist CNQX, the $GABA_A$ and glycine receptor antagonists bicuculline (bic) and strychnine (stry), and the NMDA receptor antagonist D-AP5, $n = 5$ slices. Top traces illustrate original population Ca^{2+} transients evoked by tetanic stimulation (time point marked by a dot) under the respective conditions. *$P < 0.05$ for comparison with the corresponding value in the absence of blockers.

Synchronized activity in the spinal dorsal horn

Previous studies in embryonal and neonatal rats (Kremer & Lev-Tov, 1998; Demir et al., 2002; Asghar et al., 2005), in young rats and mice (Czéh & Somjen, 1989; Ruscheweyh & Sandkühler, 2003) and in adult rats (Lidierth & Wall, 1996) suggest that synchronized discharges may occur in the spinal dorsal horn under conditions of enhanced neuronal excitability. A phenomenon equivalent to cortical spreading depression has also been described (Gorji et al., 2004). However, the methods used in these studies did not allow determination of the number and distribution of the neurons participating in the synchronous activity. The present study is the first to directly visualize synchronized dorsal horn activity and its spread at a cellular resolution. It turned out that synchronous network activity was induced by blockade of $GABA_A$ and glycine receptors, was greatly enhanced by the addition of 4-AP, and further stabilized by blockade of AMPA/kainate receptors. We found that virtually every dorsal horn neuron participated in the Ca^{2+} waves that arose under these conditions. These waves of neuronal excitation were most pronounced at P10–12 and 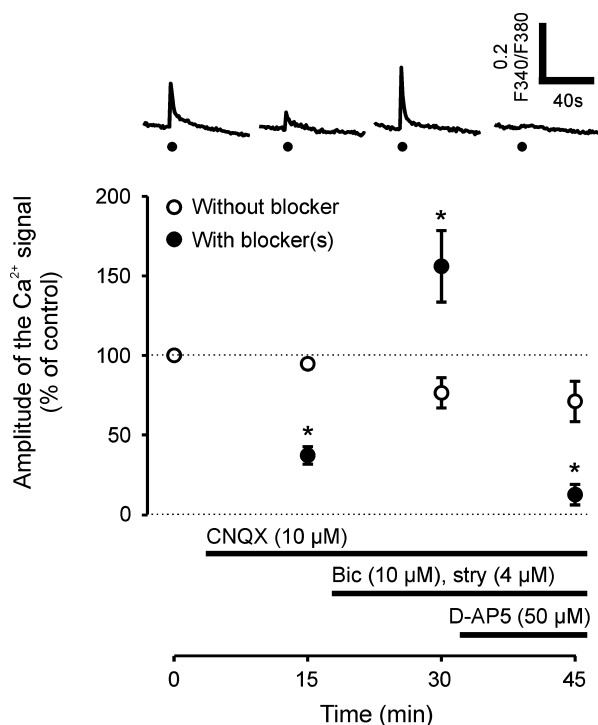reduced at P19. This may be a special feature of the presently described NMDA receptor-dependent type of network excitation (see below). The waves of excitation also spread to the contralateral dorsal horn, and we present evidence that GABAergic and/or glycinergic inhibition prevent the spread of excitation to the contralateral dorsal horn under normal conditions. GABA and glycine have previously been reported to govern the communication between right and left ventral horn (Butt et al., 2002).

Classification of Ca^{2+} waves

Ca^{2+} waves have been classified according to their synaptic or nonsynaptic propagation, their dependence on intracellular Ca^{2+} stores and their speed of propagation (Jaffe, 1993, 2002; Berridge & Dupont, 1994; Charles et al., 1996). The Ca^{2+} waves described in the present study were independent of intracellular Ca^{2+} stores, and their propagation seemed to rely on chemical synaptic transmission, as they were abolished by blockers of action potential generation or NMDA receptors. Consistent with spread by chemical synaptic transmission, their speed of propagation was fast (about 1 mm/s). This falls in between the fast and ultrafast Ca^{2+} waves as classified by Jaffe (2002), and is similar to the propagation speed of synaptically mediated Ca^{2+} or depolarizing waves found in the neocortex (Wong & Prince, 1990; Garaschuk et al., 2000; Peinado, 2001).

Spontaneous or facilitated population Ca^{2+} waves have been described and classified in many parts of the CNS (Yuste *et al.*, 1995; Feller *et al.*, 1996; Garaschuk *et al.*, 1998, 2000). Ca^{2+}-imaging is a reliable tool to monitor the activity of populations of neurons at single-cell resolution. As most neurons possess somatic voltage-gated Ca^{2+} channels, every membrane depolarization reaching the threshold for these channels causes a Ca^{2+} influx visible by Ca^{2+}-imaging. Direct visualization of membrane depolarization in populations of neurons is technically possible, but requires massive averaging precluding its use for spontaneously occurring events, and single-cell resolution is not always reached (Ikeda *et al.*, 2003). Thus, in many studies, including the present one, Ca^{2+} waves are used as an indicator of spreading neuronal excitation (Darbon *et al.*, 2002; Cossart *et al.*, 2005).

NMDA receptor dependency of the Ca²⁺ waves

The presently described Ca^{2+} waves were most pronounced in superficial dorsal horn with a decreasing intensity towards deeper laminae and they were absent in ventral horn. In addition, they were not limited to but most easily evoked during a developmental time window. As the Ca^{2+} waves were highly dependent on NMDA receptors, a differential distribution of these receptors or their subtypes could be responsible for this. Indeed, anatomical studies found a differential distribution of NMDA receptors and their subunits among laminae, often with a concentration in the superficial dorsal horn (Kalb *et al.*, 1992; Tölle *et al.*, 1993; Watanabe *et al.*, 1994; Nagy *et al.*, 2004). A developmental decrease of receptors has been reported (Kalb *et al.*, 1992; Monyer *et al.*, 1994), and pharmacologically different immature and mature types of NMDA receptors have been suggested (Sircar, 2000).

The present data show that superficial dorsal horn NMDA receptors open in response to glutamate in the absence of functional AMPA/kainate receptors at resting membrane potential and at normal Mg^{2+} concentrations. Thus, the Mg^{2+} block seems to be relatively weak in these receptors. NMDA receptors containing the NR2C or NR2D subunits exhibit low sensitivity to Mg^{2+} (Monyer *et al.*, 1994), and the NR2C subunit is concentrated in the superficial dorsal horn (Tölle *et al.*, 1993). Similar to our results, other investigators have found that purely NMDA receptor-mediated responses can be evoked in superficial dorsal horn cells at resting membrane potential in the presence of Mg^{2+} (Reichling & MacDermott, 1996; Bardoni *et al.*, 2000; Wang & Zhuo, 2002), raising the question if 'silent synapses' (i.e. synapses containing NMDA receptors but no AMPA receptors) in superficial spinal dorsal horn (Li & Zhuo, 1998; Baba *et al.*, 2000) are really 'silent' at resting membrane potential.

Possible implications of the spread of excitation over the spinal dorsal horn

The present results show that the spinal dorsal horn possesses a network structure that in principle allows the spread of excitation from a focus to the remainder of the ipsilateral and contralateral dorsal horns. This is an interesting result in view of the arrangement of sensory modalities and somatotopic origins in dorsal horn. Primary afferents and interneurons processing information from different somatotopic origins are arranged mediolaterally, while sensory modalities, e.g. the senses of touch and pain, are associated with dorsal horn lamination (Willis & Coggeshall, 2004). These different types of information have to be effectively kept separate for the benefit of orderly information processing, but the exact mechanism of this separation is not known. The fact that excitation can spread from a focus over the remainder of the dorsal horn shows that dorsal horn topological order and modality specificity are not assured anatomically, but need to be actively maintained, and can be overcome by reduced inhibition and increased excitability. Interestingly, reduced inhibition and increased neuronal excitability are present in dorsal horns of animals with neuropathic pain (Laird & Bennett, 1993; Woolf, 2004), and neuropathic pain is characterized by violation of sensory modality borders (e.g. allodynia, where normally non-noxious stimuli are perceived as painful) and somatotopic borders (radiating pain or mirror-image pain) (Maleki *et al.*, 2000; Jensen *et al.*, 2001). In the present study, crossing of somatotopic and sensory modality borders in spinal dorsal horn was observed during complete blockade of GABAergic and glycinergic inhibition and a strong promoter of excitability, conditions that are not likely to occur in neuropathic animals. Further studies, including studies in neuropathic animals, will be needed to evaluate under what physiological and pathophysiological conditions crossing of somatotopic and sensory modality borders occurs in spinal dorsal horn. However, there are several hints that reduced GABAergic and/or glycinergic inhibition may be important factors. First, reduction of spinal dorsal horn GABAergic and glycinergic inhibition has been found in animal models of long-lasting pain (Ibuki *et al.*, 1997; Moore *et al.*, 2002; Müller *et al.*, 2003). Second, intrathecal application of the GABA$_A$ receptor antagonist bicuculline or the glycine receptor antagonist strychnine in the rat leads to tactile allodynia (Yaksh, 1989; Sivilotti & Woolf, 1994). Third, in the present study, GABA and/or glycinergic inhibition also prevented the spread of excitation to the contralateral dorsal horn, showing that it has a role in shaping and containment of neuronal activity.

Acknowledgements

Abbreviations

4-AP, 4-aminopyridine; AMPA, (RS)-alpha-amino-3-hydroxy-5-methyl-4-isoxazolepropionic acid; CNQX, 6-cyano-7-nitro-quinoxaline-2,3-dione; D-AP5, D-2-amino-5-phosphonovaleric acid; fura-2 AM, fura 2 acetoxymethyl ester; GABA, γ-aminobutyric acid; NMDA, *N*-methyl-D-aspartate; P, postnatal day; TTX, tetrodotoxin.

References

Aram, J.A., Michelson, H.B. & Wong, R.K. (1991) Synchronized GABAergic IPSPs recorded in the neocortex after blockade of synaptic transmission mediated by excitatory amino acids. *J. Neurophysiol.*, **65**, 1034–1041.

Asghar, A.U., Cilia La Corte, P.F., LeBeau, F.E., Al Dawoud, M., Reilly, S.C., Buhl, E.H., Whittington, M.A. & King, A.E. (2005) Oscillatory activity within rat substantia gelatinosa *in vitro*: a role for chemical and electrical neurotransmission. *J. Physiol.*, **562**, 183–198.

Baba, H., Doubell, T.P., Moore, K.A. & Woolf, C.J. (2000) Silent NMDA receptor-mediated synapses are developmentally regulated in the dorsal horn of the rat spinal cord. *J. Neurophysiol.*, **83**, 955–962.

Bardoni, R., Magherini, P.C. & MacDermott, A.B. (2000) Activation of NMDA receptors drives action potentials in superficial dorsal horn from neonatal rats. *Neuroreport*, **11**, 1721–1727.

Berridge, M.J. & Dupont, G. (1994) Spatial and temporal signalling by calcium. *Curr. Opin. Cell Biol.*, **6**, 267–274.

Bracci, E., Ballerini, L. & Nistri, A. (1996) Localization of rhythmogenic networks responsible for spontaneous bursts induced by strychnine and bicuculline in the rat isolated spinal cord. *J. Neurosci.*, **16**, 7063–7076.

Bregestovski, P. & Spitzer, N. (2005) Calcium in the function of the nervous system: new implications. *Cell Calcium*, **37**, 371–374.

Butt, S.J., Lebret, J.M. & Kiehn, O. (2002) Organization of left-right coordination in the mammalian locomotor network. *Brain Res. Brain Res. Rev.*, **40**, 107–117.

Charles, A.C., Kodali, S.K. & Tyndale, R.F. (1996) Intercellular calcium waves in neurons. *Mol. Cell Neurosci.*, **7**, 337–353.

Cossart, R., Ikegaya, Y. & Yuste, R. (2005) Calcium imaging of cortical networks dynamics. *Cell Calcium*, **37**, 451–457.

Czéh, G. & Somjen, G.G. (1989) Spontaneous activity induced in isolated mouse spinal cord by high extracellular calcium and by low extracellular magnesium. *Brain Res.*, **495**, 89–99.

Darbon, P., Pignier, C., Niggli, E. & Streit, J. (2002) Involvement of calcium in rhythmic activity induced by disinhibition in cultured spinal cord networks. *J. Neurophysiol.*, **88**, 1461–1468.

Demir, R., Gao, B.X., Jackson, M.B. & Ziskind-Conhaim, L. (2002) Interactions between multiple rhythm generators produce complex patterns of oscillation in the developing rat spinal cord. *J. Neurophysiol.*, **87**, 1094–1105.

Dodt, H.U., Frick, A., Kampe, K. & Zieglgänsberger, W. (1998) NMDA and AMPA receptors on neocortical neurons are differentially distributed. *Eur. J. Neurosci.*, **10**, 3351–3357.

Feller, M.B. (1999) Spontaneous correlated activity in developing neural circuits. *Neuron*, **22**, 653–656.

Feller, M.B., Wellis, D.P., Stellwagen, D., Werblin, F.S. & Shatz, C.J. (1996) Requirement for cholinergic synaptic transmission in the propagation of spontaneous retinal waves. *Science*, **272**, 1182–1187.

Garaschuk, O., Hanse, E. & Konnerth, A. (1998) Developmental profile and synaptic origin of early network oscillations in the CA1 region of rat neonatal hippocampus. *J. Physiol.*, **507**, 219–236.

Garaschuk, O., Linn, J., Eilers, J. & Konnerth, A. (2000) Large-scale oscillatory calcium waves in the immature cortex. *Nat. Neurosci.*, **3**, 452–459.

Gorji, A., Zahn, P.K., Pogatzki, E.M. & Speckmann, E.J. (2004) Spinal and cortical spreading depression enhance spinal cord activity. *Neurobiol. Dis.*, **15**, 70–79.

Hanse, E., Durand, G.M., Garaschuk, O. & Konnerth, A. (1997) Activity-dependent wiring of the developing hippocampal neuronal circuit. *Semin. Cell Dev. Biol.*, **8**, 35–42.

Ibuki, T., Hama, A.T., Wang, X.T., Pappas, G.D. & Sagen, J. (1997) Loss of GABA-immunoreactivity in the spinal dorsal horn of rats with peripheral nerve injury and promotion of recovery by adrenal medullary grafts. *Neuroscience*, **76**, 845–858.

Ikeda, H., Kusudo, K., Ryu, P.D. & Murase, K. (2003) Effects of corticotropin-releasing factor on plasticity of optically recorded neuronal activity in the substantia gelatinosa of rat spinal cord slices. *Pain*, **106**, 197–207.

Jaffe, L.F. (1993) Classes and mechanisms of calcium waves. *Cell Calcium*, **14**, 736–745.

Jaffe, L.F. (2002) On the conservation of fast calcium wave speeds. *Cell Calcium*, **32**, 217–229.

Jensen, T.S., Gottrup, H., Sindrup, S.H. & Bach, F.W. (2001) The clinical picture of neuropathic pain. *Eur. J. Pharmacol.*, **429**, 1–11.

Kalb, R.G., Lidow, M.S., Halsted, M.J. & Hockfield, S. (1992) N-methyl-D-aspartate receptors are transiently expressed in the developing spinal cord ventral horn. *Proc. Natl. Acad. Sci. USA*, **89**, 8502–8506.

Katz, L.C. & Shatz, C.J. (1996) Synaptic activity and the construction of cortical circuits. *Science*, **274**, 1133–1138.

Kremer, E. & Lev-Tov, A. (1998) GABA-receptor-independent dorsal root afferents depolarization in the neonatal rat spinal cord. *J. Neurophysiol.*, **79**, 2581–2592.

Laird, J.M. & Bennett, G.J. (1993) An electrophysiological study of dorsal horn neurons in the spinal cord of rats with an experimental peripheral neuropathy. *J. Neurophysiol.*, **69**, 2072–2085.

Li, P. & Zhuo, M. (1998) Silent glutamatergic synapses and nociception in mammalian spinal cord. *Nature*, **393**, 695–698.

Lidierth, M. & Wall, P.D. (1996) Synchronous inherent oscillations of potentials within the rat lumbar spinal cord. *Neurosci. Lett.*, **220**, 25–28.

Maleki, J., LeBel, A.A., Bennett, G.J. & Schwartzman, R.J. (2000) Patterns of spread in complex regional pain syndrome, type I (reflex sympathetic dystrophy). *Pain*, **88**, 259–266.

Monyer, H., Burnashev, N., Laurie, D.J., Sakmann, B. & Seeburg, P.H. (1994) Developmental and regional expression in the rat brain and functional properties of four NMDA receptors. *Neuron*, **12**, 529–540.

Moore, K.A., Kohno, T., Karchewski, L.A., Scholz, J., Baba, H. & Woolf, C.J. (2002) Partial peripheral nerve injury promotes a selective loss of GABAergic inhibition in the superficial dorsal horn of the spinal cord. *J. Neurosci.*, **22**, 6724–6731.

Müller, F., Heinke, B. & Sandkühler, J. (2003) Reduction of glycine receptor-mediated miniature inhibitory postsynaptic currents in rat spinal lamina I neurons after peripheral inflammation. *Neuroscience*, **122**, 799–805.

Müller, W. & Misgeld, U. (1991) Picrotoxin- and 4-aminopyridine-induced activity in hilar neurons in the guinea pig hippocampal slice. *J. Neurophysiol.*, **65**, 141–147.

Nagy, G.G., Watanabe, M., Fukaya, M. & Todd, A.J. (2004) Synaptic distribution of the NR1, NR2A and NR2B subunits of the N-methyl-D-aspartate receptor in the rat lumbar spinal cord revealed with an antigen-unmasking technique. *Eur. J. Neurosci.*, **20**, 3301–3312.

O'Donovan, M.J., Bonnot, A., Wenner, P. & Mentis, G.Z. (2005) Calcium imaging of network function in the developing spinal cord. *Cell Calcium*, **37**, 443–450.

Peinado, A. (2001) Immature neocortical neurons exist as extensive syncitial networks linked by dendrodendritic electrical connections. *J. Neurophysiol.*, **85**, 620–629.

Reichling, D.B. & MacDermott, A.B. (1996) NMDA receptor-mediated calcium entry in the absence of AMPA receptor activation in rat dorsal horn neurons. *Neurosci. Lett.*, **204**, 17–20.

Ruscheweyh, R. & Sandkühler, J. (2002) Lamina-specific membrane and discharge properties of rat spinal dorsal horn neurones *in vitro*. *J. Physiol.*, **541**, 231–244.

Ruscheweyh, R. & Sandkühler, J. (2003) Epileptiform activity in rat spinal dorsal horn *in vitro* has common features with neuropathic pain. *Pain*, **105**, 327–338.

Sircar, R. (2000) Developmental maturation of the N-methyl-D-aspartic acid receptor channel complex in postnatal rat brain. *Int. J. Dev. Neurosci.*, **18**, 121–131.

Sivilotti, L. & Woolf, C.J. (1994) The contribution of GABA$_A$ and glycine receptors to central sensitization: disinhibition and touch-evoked allodynia in the spinal cord. *J. Neurophysiol.*, **72**, 169–179.

Tölle, T.R., Berthele, A., Zieglgänsberger, W., Seeburg, P.H. & Wisden, W. (1993) The differential expression of 16 NMDA and non-NMDA receptor subunits in the rat spinal cord and in periaqueductal gray. *J. Neurosci.*, **13**, 5009–5028.

Wang, G.D. & Zhuo, M. (2002) Synergistic enhancement of glutamate-mediated responses by serotonin and forskolin in adult mouse spinal dorsal horn neurons. *J. Neurophysiol.*, **87**, 732–739.

Watanabe, M., Mishina, M. & Inoue, Y. (1994) Distinct spatiotemporal distributions of the N-methyl-D-aspartate receptor channel subunit mRNAs in the mouse cervical cord. *J. Comp. Neurol.*, **345**, 314–319.

Willis, W.D. Jr & Coggeshall, R.E. (2004) *Sensory Mechanisms of the Spinal Cord. Primary Afferent Neurons and the Spinal Dorsal Horn*. Kluwer Academic, New York.

Wong, B.Y. & Prince, D.A. (1990) The lateral spread of ictal discharges in neocortical brain slices. *Epilepsy Res.*, **7**, 29–39.

Woolf, C.J. (2004) Dissecting out mechanisms responsible for peripheral neuropathic pain: implications for diagnosis and therapy. *Life Sci.*, **74**, 2605–2610.

Yaksh, T.L. (1989) Behavioral and autonomic correlates of the tactile evoked allodynia produced by spinal glycine inhibition: effects of modulatory receptor systems and excitatory amino acid antagonists. *Pain*, **37**, 111–123.

Yuste, R., Nelson, D.A., Rubin, W.W. & Katz, L.C. (1995) Neuronal domains in developing neocortex: mechanisms of coactivation. *Neuron*, **14**, 7–17.